

Translational Diffusion in Lipid Membranes beyond the Saffman-Delbrück Approximation

Eugene P. Petrov and Petra Schille

Biophysics, BIOTEC, Technische Universität Dresden, 01307 Dresden, Germany

ABSTRACT The Saffman-Delbrück approximation is commonly used in biophysics to relate the membrane inclusion size to its translational diffusion coefficient and membrane viscosity. However, this approximation has a restricted validity range, and its application to determination of inclusion sizes from diffusion data may in certain cases lead to unreliable results. At the same time, the model by Hughes et al. (Hughes, B. D., B. A. Pailthorpe, and C. R. White. 1981. *J. Fluid Mech.* 110:349–372.), providing diffusion coefficients of membrane inclusions for arbitrary inclusion sizes and viscosities of the membrane and surrounding fluids, involves substantial computational efforts, which prevents its use in practical data analysis. We develop a simple and accurate analytical approximation to the Hughes et al. model and demonstrate its performance and utility by applying it to the recently published experimental data on translational diffusion of micrometer-sized membrane domains.

Received for publication 28 November 2007 and in final form 28 December 2007.

Address reprint requests and inquiries to Eugene P. Petrov, E-mail: petrov@biotec.tu-dresden.de.

During the last decade, the concept of lipid rafts (1)—submicrometer-sized functional lipid domains on cell membranes—has attracted considerable attention in view of the important role they may play in cell functioning (2). Though there is no universal agreement on whether rafts show translational diffusion, attempts have been made to estimate the raft dimensions from diffusion coefficients of raft-associated proteins (3). Thus, a better understanding of raft dynamics requires information on the membrane viscosity and its dependence on the membrane composition and temperature. This information can be obtained by, e.g., single-particle tracking (4), fluorescence recovery after photobleaching (5), fluorescence correlation spectroscopy (6), or NMR (7). Additionally, it is important to correctly relate measured translational diffusion coefficients of membrane inclusions to their sizes.

Traditionally, data on diffusion of membrane inclusions are related to inclusion sizes using the Saffman-Delbrück (SD) model (8,9). It comprises a leading-order approximate solution of the hydrodynamic problem (10) of translational motion of an inclusion in a membrane surrounded by a viscous fluid. The SD approximation was originally developed to explain protein mobility in membranes, and is therefore valid only for membrane inclusions that are small compared to the characteristic length scale brought about by hydrodynamics (see below). In spite of that, the SD approximation is widely used in membrane studies, including the analysis of simulated (11) and experimental (12) data on membrane domain diffusion, where, not surprisingly, it was found to fail at certain inclusion sizes and membrane viscosities.

In fact, a hydrodynamic model describing the mobility of a membrane inclusion of an arbitrary radius for arbitrary viscosities of the membrane and surrounding media was developed in 1981 by Hughes, Pailthorpe, and White (HPW)

(13). However, the HPW model involves complicated numerical computations, which prevents its direct practical applications.

In this Letter, we propose a simple analytical expression for the diffusion coefficient of a membrane inclusion providing a high-accuracy approximation of the HPW results, which can be easily used to analyze membrane diffusion data and relate measured diffusion coefficients to the inclusion size and membrane viscosity. To demonstrate the utility and performance of our approximation, we apply it to recent experimental data (12) on diffusion of micrometer-sized domains in phospholipid membranes.

In the hydrodynamic description, the cylindrical inclusion of radius a is embedded in a membrane with the surface viscosity η (14), which is surrounded by media with bulk viscosities μ_1 and μ_2 (see sketch in Fig. 1). The corresponding hydrodynamic length scale is $l = \eta/(\mu_1 + \mu_2)$ (13), and the membrane inclusion is characterized by the reduced radius $\varepsilon = a/l = a(\mu_1 + \mu_2)/\eta$. The translational diffusion coefficient of the membrane inclusion can be expressed as $D(\varepsilon) = D_0\Delta(\varepsilon)$, where $D_0 = k_B T/(4\pi\eta)$, and $\Delta(\varepsilon)$ is the reduced mobility.

The reduced mobility $\Delta_{\text{HPW}}(\varepsilon)$ according to the exact solution of the HPW model (13) is shown in Fig. 1. To compute $\Delta_{\text{HPW}}(\varepsilon)$ within a wide range of ε , we transformed the integral equation Eq. 3.36 of HPW (13) into an infinite system of linear equations along the lines described in Eqs. 3.43–3.49 of HPW (13). Integrals involving products of Bessel functions were evaluated numerically using the approach described in Lucas (15) with the convergence acceleration method of Cohen et al. (16). Truncating the

Editor: Michael Edidin.

© 2008 by the Biophysical Society
doi: 10.1529/biophysj.107.126565

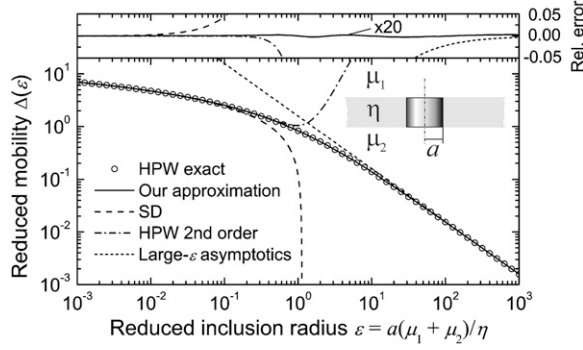


FIGURE 1 Reduced membrane inclusion mobility: the exact HPW result $\Delta_{\text{HPW}}(\varepsilon)$ (circles), SD approximation $\hat{\Delta}_{\text{SD}}(\varepsilon)$ (dashed curve), HPW second-order approximation $\hat{\Delta}_{\text{HPW}}^{(2)}(\varepsilon)$ (dash-dotted curve), the large- ε asymptotics $\hat{\Delta}_{\text{HPW},\infty}(\varepsilon)$ (dotted line), and the proposed approximation $\hat{\Delta}(\varepsilon)$ (solid curve). All curves are computed under the assumption of the no-slip condition at the inclusion boundary (21). The upper panel shows the relative errors of the corresponding approximations.

system to 30 equations was found to provide stable and accurate results.

In the SD approximation (8,9,13), the reduced mobility $\hat{\Delta}_{\text{SD}}(\varepsilon) = \ln(2/\varepsilon) - \gamma$, with $\gamma = 0.577215$ being the Euler constant, is expected to reproduce well the exact HPW solution when $\varepsilon = a/l \ll 1$. As is clear from Fig. 1, the SD model indeed provides a good approximation of $\Delta_{\text{HPW}}(\varepsilon)$ for $\varepsilon < 0.1$. The second-order approximation introduced in HPW (13) $\hat{\Delta}_{\text{HPW}}^{(2)}(\varepsilon) = \ln(2/\varepsilon) - \gamma + 4\varepsilon/\pi - (\varepsilon^2/2)\ln(2/\varepsilon)$ has a somewhat extended applicability range of $\varepsilon < 0.6$ (Fig. 1). At large ε , the reduced mobility of the membrane inclusion behaves asymptotically as (13) $\hat{\Delta}_{\text{HPW},\infty}(\varepsilon) = \pi/(2\varepsilon)$. This asymptotic behavior, which was confirmed experimentally in Klingler et al. (17), is achieved only for $\varepsilon > \sim 30$ (Fig. 1).

Fig. 1 clearly shows that application of the above approximations outside their validity ranges can lead to a bias in inclusion size determination from diffusion data. For example, for a membrane with $\eta \approx 4 \times 10^{-10}$ Pa·s·m (18), surrounded by fluids with $\mu_{1,2} \approx 10^{-3}$ Pa·s, a membrane inclusion with $a = 100$ nm will be characterized by $\varepsilon \approx 0.5$. In this case, the use of the SD approximation in diffusion data analysis would yield $a = 65$ nm, which is a factor of 1.5 smaller than the real inclusion size. In cases where $\varepsilon > \sim 1$, the SD approximation fails completely and is therefore useless in membrane diffusion analysis.

Our goal is to develop a simple and accurate analytical approximation $\hat{\Delta}(\varepsilon)$ of $\Delta_{\text{HPW}}(\varepsilon)$ valid for the whole range of the reduced inclusion radius ε . We notice that the ratio $\varphi(\varepsilon) = \Delta_{\text{HPW}}(\varepsilon)/\hat{\Delta}_{\text{HPW}}^{(2)}(\varepsilon)$ is nonnegative and monotonically decays from one to zero when ε increases from zero to infinity. Therefore, we can describe $\Delta_{\text{HPW}}(\varepsilon)$ by constructing an approximation $\hat{\varphi}(\varepsilon)$ for $\varphi(\varepsilon)$, which would satisfy the following asymptotic conditions: $\hat{\varphi}(\varepsilon) \simeq 1$, $\varepsilon \rightarrow 0$; $\hat{\varphi}(\varepsilon) \simeq -[(\varepsilon^3/\pi)\ln(2/\varepsilon)]^{-1}$, $\varepsilon \rightarrow \infty$. We have found that the following expression $\hat{\varphi}(\varepsilon) = [1 - (\varepsilon^3/\pi)\ln(2/\varepsilon) + c_1\varepsilon^{b_1}/(1 + c_2\varepsilon^{b_2})]^{-1}$

with the parameters $c_1 = 0.73761$, $b_1 = 2.74819$, $c_2 = 0.52119$, and $b_2 = 0.61465$ excellently serves this purpose (19). The resulting approximation for the reduced mobility of a cylindrical inclusion in a membrane, $\hat{\Delta}(\varepsilon) = \hat{\Delta}_{\text{HPW}}^{(2)}(\varepsilon)\hat{\varphi}(\varepsilon)$, describes $\Delta_{\text{HPW}}(\varepsilon)$ within the whole range of ε with the relative error below 0.015% (Fig. 1). For convenience, we provide the explicit form of our approximation for the diffusion coefficient of a membrane inclusion:

$$\begin{aligned} \hat{D}(\varepsilon) &= k_B T / (4\pi\eta) \\ &\times [\ln(2/\varepsilon) - \gamma + 4\varepsilon/\pi - (\varepsilon^2/2)\ln(2/\varepsilon)] \\ &\times [1 - (\varepsilon^3/\pi)\ln(2/\varepsilon) + c_1\varepsilon^{b_1}/(1 + c_2\varepsilon^{b_2})]^{-1}. \end{aligned} \quad (1)$$

The approximation Eq. 1 fully satisfies our goals: it reproduces the exact solution of the HPW model with a high accuracy within the whole range of ε and is simple enough to be applied directly in data analysis without a danger of obtaining biased results due to the use of an approximation outside its applicability range.

To illustrate the performance and utility of our approximation, we apply it to the recent experimental results (12) on diffusion of micrometer-sized domains in phospholipid membranes (for details, see the original article). In particular, we analyze data sets for diffusion of liquid-crystalline (L_α) domains in the liquid-ordered (L_o) phase of giant unilamellar vesicles with the composition 1:2 DOPC/DPPC + 30% cholesterol and 1:1 DOPC/DPPC + 30% cholesterol at a range of temperatures. The viscosity of the surrounding medium is described using the standardized data on water viscosity (20).

In Cicuta et al. (12), the diffusion data were analyzed using the SD approximation, which restricted the analysis to lower-temperature data sets. Indeed, we found that, although the SD approximation could provide a reasonable description of lower-temperature data ($t < 20^\circ\text{C}$) (see Fig. 2), it completely failed to describe data measured at $t \geq 20^\circ\text{C}$. Additionally, for the data set of $t = 16^\circ\text{C}$ in Fig. 2 b, a reasonable SD fit could

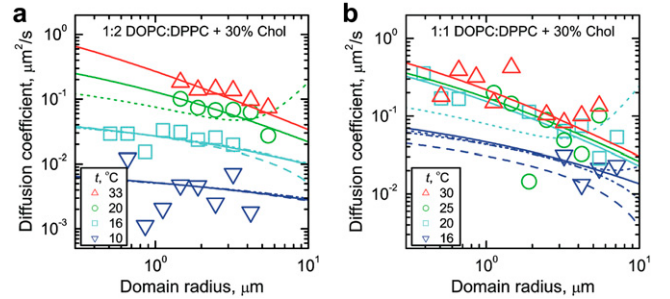


FIGURE 2 Diffusion coefficients of membrane domains from Cicuta et al. (12) for a range of temperatures (symbols) and their fits using our approximation Eq. 1 of the HPW model (solid curves). Fits of several data sets with the SD model assuming no-slip (dashed curves) and slip (dash-dot-dot curves) boundary conditions at the inclusion boundary (see text), and with the second-order HPW approximation (dotted curves) are shown. Membrane compositions: 1:2 DOPC/DPPC + 30% cholesterol (a); 1:1 DOPC/DPPC + 30% cholesterol (b).

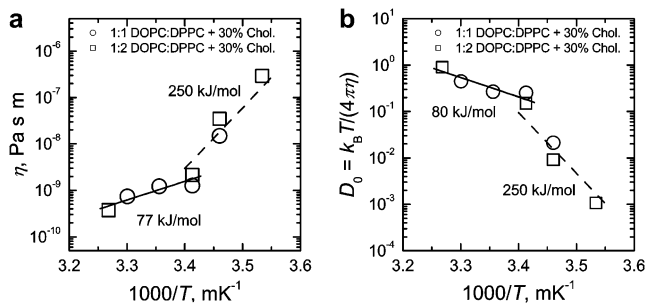


FIGURE 3 Arrhenius dependences of the surface membrane viscosity η (a) and size-independent diffusion coefficient D_0 (b) recovered from the analysis of data shown in Fig. 2 using our approximation: 1:1 DOPC/DPPC + 30% cholesterol (circles) and 1:2 DOPC/DPPC + 30% cholesterol (squares). (Dashed lines) Arrhenius dependences from Cicuta et al. (12) for data at $t \leq 20^\circ\text{C}$. (Solid lines) Arrhenius fits for data at $t \geq 20^\circ\text{C}$.

only be obtained assuming the slip boundary conditions (21). Clearly, the second-order HPW approximation also fails to provide adequate fits to data at $t \geq 20^\circ\text{C}$. By contrast, our approximation Eq. 1 adequately describes the diffusion data within the whole temperature range (Fig. 2).

Arrhenius plots for the membrane surface viscosity η recovered by fitting the data with Eq. 1 and the corresponding size-independent diffusion coefficient $D_0 = k_B T / (4\pi\eta)$ are shown in Fig. 3. As in Cicuta et al. (12), we found very similar values of η and D_0 for the membrane compositions 1:2 DOPC/DPPC + 30% cholesterol and 1:1 DOPC/DPPC + 30% cholesterol. In Cicuta et al. (12), the analysis of data restricted to the temperature range of $t \leq 20^\circ\text{C}$ gave the activation energy of ~ 250 kJ/mol, which is substantially higher than the previously reported activation energies of 55–65 kJ/mol for the L_o membrane phase (22). However, the activation energies in Filippov et al. (22) were determined from data at temperatures $t > 20^\circ\text{C}$, and therefore a direct comparison of these values with the results for $t \leq 20^\circ\text{C}$ might not be fully justified. At the same time, application of our approximation Eq. 1 to data (12) at $t \geq 20^\circ\text{C}$ recovers η and D_0 showing the activation energy of ~ 80 kJ/mol, in good agreement with the previously reported data (22).

ACKNOWLEDGMENTS

The authors are grateful to Dr. S. L. Veatch for kindly providing the original experimental data.

The work was supported by the Deutsche Forschungsgemeinschaft via Research Unit 877 “From Local Constraints to Macroscopic Transport”.

REFERENCES and FOOTNOTES

1. Simons, K., and E. Ikonen. 1997. Functional rafts in cell membranes. *Nature*. 387:569–572.

2. Jacobson, K., O. G. Mouritsen, and R. G. W. Anderson. 2007. Lipid rafts: at a crossroad between cell biology and physics. *Nat. Cell Biol.* 9:7–14.
3. Pralle, A., P. Keller, E.-L. Florin, K. Simons, and J. K. H. Hörber. 2000. Sphingolipid-cholesterol rafts diffuse as small entities in the plasma membrane of mammalian cells. *J. Cell Biol.* 148:997–1007.
4. Saxton, M. J., and K. Jacobson. 1997. Single-particle tracking: Applications to membrane dynamics. *Annu. Rev. Biophys. Biomol. Struct.* 26:373–399.
5. Yguerabide, J., J. A. Schmidt, and E. E. Yguerabide. 1982. Lateral mobility in membranes as detected by fluorescence recovery after photobleaching. *Biophys. J.* 40:69–75.
6. Bacia, K., D. Scherfeld, N. Kahya, and P. Schwille. 2004. Fluorescence correlation spectroscopy relates rafts in model and native membranes. *Biophys. J.* 87:1034–1043.
7. Orädd, G., and G. Lindblom. 2004. Lateral diffusion studied by pulsed field gradient NMR on oriented lipid membranes. *Magn. Reson. Chem.* 42:123–131.
8. Saffman, P. G., and M. Delbrück. 1975. Brownian motion in biological membranes. *Proc. Natl. Acad. Sci. USA*. 72:3111–3113.
9. Saffman, P. G. 1976. Brownian motion in thin sheets of viscous fluid. *J. Fluid Mech.* 73:593–602.
10. The hydrodynamic description implies that the membrane inclusion size is much larger than that of the lipid headgroup—the condition assumed to be always satisfied in this study.
11. Guigas, G., and M. Weiss. 2006. Size-dependent diffusion of membrane inclusions. *Biophys. J.* 91:2393–2398.
12. Cicuta, P., S. L. Keller, and S. L. Veatch. 2007. Diffusion of liquid domains in lipid bilayer membranes. *J. Phys. Chem. B*. 111:3328–3331.
13. Hughes, B. D., B. A. Pailthorpe, and L. R. White. 1981. The translational and rotational drag on a cylinder moving in a membrane. *J. Fluid Mech.* 110:349–372.
14. For a homogeneous membrane, its surface viscosity η (measured in Pa·s·m) can be related to the bulk viscosity of the membrane material μ (measured in Pa·s) and membrane thickness h : $\eta = \mu h$.
15. Lucas, S. K. 1995. Evaluating infinite integrals involving products of Bessel functions of arbitrary order. *J. Comput. Appl. Math.* 64:269–282.
16. Cohen, H., F. R. Villegas, and D. Zagier. 2000. Convergence acceleration of alternating series. *Exp. Math.* 9:3–12.
17. Klingler, J. F., and H. M. McConnell. 1993. Brownian motion and fluid mechanics of lipid monolayer domains. *J. Phys. Chem.* 97:6096–6100.
18. Peters, R., and R. J. Cherry. 1982. Lateral and rotational diffusion of bacteriorhodopsin in lipid bilayers: Experimental test of the Saffman-Delbrück equations. *Proc. Natl. Acad. Sci. USA*. 79:4317–4321.
19. In this expression, the first two terms in the square brackets ensure the correct limiting behavior of $\hat{\phi}(\varepsilon)$ (and hence, of $\hat{\Delta}(\varepsilon)$) at $\varepsilon \rightarrow 0, +\infty$; the third term, which in this case should tend to zero for $\varepsilon \rightarrow 0$ and grow slower than $\varepsilon^3 \ln \varepsilon$ for large ε , was chosen empirically to provide correct bridging between the two regimes. The values of the parameters $b_{1,2}$ and $c_{1,2}$ were determined by numerical minimization of the sum of squared residuals $\sum_i (\ln \phi(\varepsilon_i) - \ln \hat{\phi}(\varepsilon_i))^2$ on a grid of 161 uniformly log-spaced ε -values covering the range of $10^{-3} \dots 10^5$.
20. Kestin, J., M. Sokolov, and W. A. Wakeham. 1978. Viscosity of liquid water in the range -8°C to 150°C . *J. Phys. Chem. Ref. Data*. 7:941–948.
21. Theoretically, for liquid membrane domains, the slip boundary condition should be more appropriate, in which case the SD approximation is $\Delta_{SD, \text{slip}}(\varepsilon) = \ln(2/\varepsilon) - \gamma + 1/2$ (see Saffman (9)). In practice, however, one may still expect the no-slip boundary condition, as it usually takes place for liquid droplets moving in bulk fluids. See, e.g., Levich, V. G. 1962. *Physicochemical Hydrodynamics*, Prentice-Hall, Englewood Cliffs, NJ.
22. Filippov, A., G. Orädd, and G. Lindblom. 2003. The effect of cholesterol on the lateral diffusion of phospholipids in oriented bilayers. *Biophys. J.* 84:3079–3086.